ACS APPLIED MATERIALS & INTERFACES

Research Article

www.acsami.org

Origin of Outstanding Stability in the Lithium Solid Electrolyte Materials: Insights from Thermodynamic Analyses Based on First-Principles Calculations

Yizhou Zhu,[†] Xingfeng He,[†] and Yifei Mo*[,†,‡]

[†]Department of Materials Science and Engineering and [‡]University of Maryland Energy Research Center, University of Maryland, College Park, Maryland 20742, United States

Supporting Information

ABSTRACT: First-principles calculations were performed to investigate the electrochemical stability of lithium solid electrolyte materials in all-solid-state Li-ion batteries. The common solid electrolytes were found to have a limited electrochemical window. Our results suggest that the outstanding stability of the solid electrolyte materials is not thermodynamically intrinsic but is originated from kinetic stabilizations. The sluggish kinetics of the decomposition reactions cause a high overpotential leading to a nominally wide electrochemical window observed in many experiments. The decomposition products, similar to the solid-electrolyte-interphases, mitigate the extreme chemical potential from the electrodes and protect the solid electrolyte from further decompositions. With the aid of the first-principles calculations, we revealed the passivation mechanism of these decomposition interphases and quantified the extensions of the electrochemical window from the interphases. We also found that the artificial coating layers applied at the solid electrolyte and electrode interfaces have a similar effect of passivating the solid electrolyte. Our newly gained understanding provided general principles for developing solid electrolyte materials with enhanced stability and for engineering interfaces in all-solid-state Li-ion batteries.

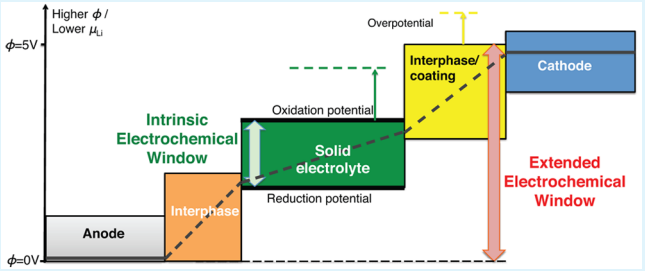

KEYWORDS: *lithium ionic conductor, solid electrolyte, electrochemical stability, passivation, solid-electrolyte-interphases, first-principles calculations*

1. INTRODUCTION

The continued drive for high energy density Li-ion batteries has imposed ever stricter requirements on the electrolyte materials. Current organic liquid electrolytes are flammable, causing notorious safety issues for Li-ion batteries. The limited electrochemical window of the organic liquid electrolytes limits the choice of electrode materials and hence the achievable energy density of the Li-ion batteries. The solid electrolyte materials based on Li-ion conducting ceramics are promising alternatives for the conventional polymer electrolytes to make all-solid-state Li-ion batteries.[1,2] Thanks to the recent discovery and development of Li ionic conductor materials such as Li thiophosphates[1,3,4] and Li garnet-type materials,[5] high Li ionic conductivities of 1−10 mS/cm comparable to the organic liquid electrolytes have been achieved in the solid electrolyte materials. Moreover, the claimed outstanding stability of ceramic solid electrolyte materials may provide intrinsic safety for the Li-ion batteries and may enable Li metal anode and high-voltage cathodes,[1,2] which may significantly increase the energy density for Li-ion batteries.[6−8]

The claimed outstanding stability of the solid electrolyte materials is based on the widely reported electrochemical window of 0−5 V from cyclic voltammetry (CV) measurements.[1,8−10] However, some recent experimental and computational studies questioned the claimed stability of solid electrolyte materials against Li metal and at high voltages. For example, the reduction and oxidation of $Li_{10}GeP_2S_{12}$ (LGPS) at low and high potentials, respectively, in contrast to the originally claimed 0−5 V electrochemical window, have been demonstrated by first-principles computation[11] and the experiments.[12] Recent in situ X-ray photoelectron spectroscopy (XPS) experiments have also observed the interfacial decomposition of LiPON,[13] lithium lanthanum titanate,[14] and NASICON-type[15] solid electrolyte materials against Li metal. These reports lead to an outstanding discrepancy, i.e., the wide electrochemical windows of 0−5 V reported in many CV experiments are contradictory to the decomposition of the solid electrolyte against Li. Although the experimental evidences for the decompositions have been reported in a range of materials from sulfides to oxides and oxynitrides, it is not clear whether the decomposition of ceramic solid electrolytes is a universal phenomenon and whether some ceramic solid electrolyte can indeed achieve a "true" stability window of 0−5 V. It is speculated that the decomposition products form interphases to

Received: August 13, 2015
Accepted: October 6, 2015
Published: October 6, 2015

DOI: 10.1021/acsami.5b07517
ACS Appl. Mater. Interfaces 2015, 7, 23685−23693

Table 1. Electrochemical Window and Phase Equilibria at the Reduction and Oxidation Potentials of the Solid Electrolyte Materials

	reduction potential (V)	phase equilibria at the reduction potential	oxidation potential (V)	phase equilibria at the oxidation potential
Li_2S	-	Li_2S (stable at 0 V)	2.01	S
LGPS	1.71	P, Li_4GeS_4, Li_2S	2.14	Li_3PS_4, GeS_2, S
$Li_{3.25}Ge_{0.25}P_{0.75}S_4$	1.71	P, Li_4GeS_4, Li_2S	2.14	Li_3PS_4, GeS_2, S
Li_3PS_4	1.71	P, Li_2S	2.31	S, P_2S_5
Li_4GeS_4	1.62	Li_2S, Ge	2.14	GeS_2, S
$Li_7P_3S_{11}$	2.28	Li_3PS_4, P_4S_9	2.31	S, P_2S_5
Li_6PS_5Cl	1.71	P, Li_2S, LiCl	2.01	Li_3PS_4, LiCl, S
$Li_7P_2S_8I$	1.71	P, Li_2S, LiI	2.31	LiI, S, P_2S_5
LiPON	0.68	Li_3P, $LiPN_2$, Li_2O	2.63	P_3N_5, $Li_4P_2O_7$, N_2
LLZO	0.05	Zr_3O, La_2O_3, Li_2O	2.91	Li_2O_2, La_2O_3, $Li_6Zr_2O_7$
LLTO	1.75	$Li_4Ti_5O_{12}$, $Li_{7/6}Ti_{11/6}O_4$, $La_2Ti_2O_7$	3.71	O_2, TiO_2, $La_2Ti_2O_7$
LATP	2.17	P, $LiTiPO_5$, $AlPO_4$, Li_3PO_4	4.21	O_2, $LiTi_2(PO_4)_3$, $Li_4P_2O_7$, $AlPO_4$
LAGP	2.70	Ge, GeO_2, $Li_4P_2O_7$, $AlPO_4$	4.27	O_2, $Ge_5O(PO_4)_6$, $Li_4P_2O_7$, $AlPO_4$
LISICON	1.44	Zn, Li_4GeO_4	3.39	Li_2ZnGeO_4, Li_2GeO_3,O_2

passivate the solid electrolytes and to inhibit the continuous bulk decompositions.[11,14,15] However, little is understood about the fundamental physical and chemical mechanisms governing the decomposition and the passivation of the solid electrolyte materials in the all-solid-state Li-ion batteries. Why only certain materials can be spontaneously passivated but others cannot? In addition, the decomposition products at the interfaces between the solid electrolyte and electrode may cause high interfacial resistances and mechanical failures in the all-solid-state Li-ion batteries.[2,16] Therefore, computation methods are needed to identify the potential formation of the interfacial decomposition products and to quantify the electrochemical window of the solid electrolyte with the considerations of the passivation effects.

In this study, we systematically investigated the electrochemical stability of common lithium solid electrolytes using first-principles computation methods. We identified the phase equilibria and decomposition reaction energies of the lithiation and delithiation of the solid electrolyte materials against Li metal and at high voltages. Our computation results determined that most solid electrolyte materials have a limited intrinsic electrochemical window and that the decomposition of most solid electrolyte materials are thermodynamically favorable forming decomposition interphases. The mechanisms were suggested regarding the origins of the high nominal electrochemical window observed in the experimental studies. In addition to the high overpotential due to the sluggish kinetics of the decomposition reactions, the passivation mechanism of the decomposition interphases were illustrated. The extensions of the electrochemical window provided by the interphases were quantified in the first-principles calculations. Similar to the interphases, the coating layer materials artificially applied at the interfaces were demonstrated to stabilize and passivate the solid electrolyte materials. These results establish general guidelines for designing solid electrolyte materials with enhanced stability, which is crucial to enable Li metal anode and high-voltage cathode materials in all-solid-state Li-ion batteries.

2. METHODS

All density functional theory (DFT) calculations in this work were performed using the Vienna Ab initio Simulation Package (VASP) within the projector augmented-wave approach, and the Perdew–Burke–Ernzerhof (PBE) generalized gradient approximation (GGA) functional was used. The parameters of DFT calculations, such as the plane-wave energy cutoff and *k*-points density, were consistent with the parameters used for the Materials Project (MP).[17] The energy correction schemes for oxides, transition metals, and gas molecules were included as in the MP.[18,19] The energies of most materials in this study were obtained from the MP database,[20] and DFT calculations were performed only for the solid electrolyte materials that were not available from the MP database. Details of these solid electrolyte structures were summarized in the Supporting Information. In addition, the calculated reaction energies and voltages neglected the contribution of the *PV* terms and the entropy terms as in previous studies.[11,21]

We constructed the grand potential phase diagram[11,21] to study the electrochemical stability of the solid electrolyte materials. The grand potential phase diagram, which were generated using *pymatgen*,[22] identified the phase equilibria of the material in equilibrium with an opening Li reservoir of Li chemical potential μ_{Li}. As in the previous studies,[11,23] the applied electrostatic potential ϕ was considered in the Li chemical potential μ_{Li} as

$$\mu_{Li}(\phi) = \mu_{Li}^{0} - e\phi \quad (1)$$

where μ_{Li}^{0} is the chemical potential of Li metal, and the potential ϕ is referenced to Li metal in this study. To quantify the thermodynamic driving force, we calculated the decomposition reaction energy E_D for the decomposition reactions at applied voltage ϕ as

$$E_D(\phi) = E(\text{phase equilibria}, \phi) - E(\text{solid electrolyte}) - \Delta n_{Li}\mu_{Li}(\phi) \quad (2)$$

where E(phase equilibria, ϕ) is the energy of the phase equilibria at the potential ϕ, E(solid electrolyte) is the energy of the solid electrolyte, and Δn_{Li} is the change of the number of Li from the solid electrolyte composition to the phase equilibria composition during the lithiation or delithation reaction.

3. RESULTS

3.1. Stability of Solid Electrolyte Materials against Li Metal. We first evaluated the electrochemical stability of solid electrolyte materials against Li metal and at low voltages. The phase equilibria, i.e., the phases with the lowest energy, in equilibrium with Li metal were identified by the Li grand potential phase diagrams (Table 1). The solid electrolyte materials are not thermodynamically stable against Li metal (Table 2) and are reduced at low voltages with highly favorable decomposition energy (Figure 1 and Table 2). In contrast, the Li binary compounds, such as LiF, Li_2O, Li_2S, Li_3P, and Li_3N, are thermodynamically stable against Li metal (Figure 2a). The lithiation and reduction of $Li_{10}GeP_2S_{12}$ (LGPS) starts at 1.71 V, and the LGPS in equilibrium with Li metal is eventually

DOI: 10.1021/acsami.5b07517
ACS Appl. Mater. Interfaces 2015, 7, 23685–23693

Table 2. Reduction Reaction of the Solid Electrolyte Materials with Li Metal

	phase equilibria with Li metal	E_D (eV/atom)
Li_2S	Li_2S (stable)	0
LGPS	$Li_{15}Ge_4$, Li_3P, Li_2S	−1.25
$Li_{3.25}Ge_{0.25}P_{0.75}S_4$	$Li_{15}Ge_4$, Li_3P, Li_2S	−1.28
Li_3PS_4	Li_3P, Li_2S	−1.42
Li_4GeS_4	$Li_{15}Ge_4$, Li_2S	−0.89
$Li_7P_3S_{11}$	Li_3P, Li_2S	−1.67
Li_6PS_5Cl	Li_3P, Li_2S, LiCl	−0.96
$Li_7P_2S_8I$	Li_3P, Li_2S, LiI	−1.26
LiPON	Li_3P, Li_3N, Li_2O	−0.66
LLZO	Zr (or Zr_3O), La_2O_3, Li_2O	−0.021
LLTO	Ti_6O, La_2O_3, Li_2O	−0.34
LATP	Ti_3P, TiAl, Li_3P, Li_2O	−1.56
LAGP	Li_9Al_4, $Li_{15}Ge_4$, Li_3P, Li_2O	−1.99
LISICON	$Li_{15}Ge_4$, LiZn, Li_2O	−0.77

lithiated into the phase equilibria consisting of $Li_{15}Ge_4$, Li_3P, and Li_2S. The Li reduction of the LGPS into these reaction products has a highly favorable reaction energy of −1.25 eV/atom (−3014 kJ/mol of LGPS) at 0 V (Figure 1 and Table 2). In agreement with our computation, the reduction of LGPS starting at 1.71 V and the formation of Li−Ge alloy after the reduction have been demonstrated in the cyclic voltammetry (CV) and XPS experiments, respectively.[12] Other sulfides materials, such as $Li_{3.25}Ge_{0.25}P_{0.75}S_4$, Li_3PS_4, Li_4GeS_4, Li_6PS_5Cl, and $Li_7P_2S_8I$, are reduced at a similar voltage of ∼1.6−1.7 V. The reduction potential is mostly governed by the reduction of P and Ge in the materials, and the reduction products include Li_3P and Li_2S at 0 V. For those materials containing Ge, Cl, and I elements, Li−Ge alloy, LiCl, and LiI are formed, respectively, as a part of phase equilibria at 0 V. The $Li_7P_3S_{11}$ is reduced at a voltage of 2.28 V into Li_3PS_4 with a small decomposition energy (Figure 1a), and the majority of the reduction starts at 1.71 V due to the lithiation of Li_3PS_4 (Table 2). The decomposition energy for all these solid electrolyte decreases with the potential to ∼−1 eV/atom at 0 V (Figure 1a and Table 2), indicating the highly favorable reduction reactions of the sulfide solid electrolytes.

The reduction of oxide solid electrolyte materials $Li_{0.33}La_{0.56}TiO_3$ (LLTO) and $Li_{1.3}Ti_{1.7}Al_{0.3}(PO_4)_3$ (LATP) starts at a voltage of 1.75 and 2.17 V, respectively. Our predicted reduction potential of LLTO is in good agreement with the value of 1.7−1.8 V reported in the CV experiments.[24,25] The calculations also found the reduction of Ti^{4+} in LLTO and LATP into Ti^{3+} or lower valences at low voltages (Tables 1 and 2). The reduction of Ti is a widely known problem and is observed at the interfaces of LLTO[14] and LATP[15] with Li metal by in situ XPS spectroscopy. In addition, the reduction of Ge-containing oxide materials $Li_{1.5}Al_{0.5}Ge_{1.5}(PO_4)_3$ (LAGP) and $Li_{3.5}Zn_{0.25}GeO_4$ (LISICON) starting at 2.7 and 1.4 V, respectively, and Li−Ge alloys are formed at low voltages (Figure 1b and Table 2). The reductions of LAGP and LISICON are consistent with the experiment studies.[26−28] The good agreements between our computation results and many experiments demonstrated the validity of our computation scheme.

Our calculations found the Li reduction of the solid electrolyte materials that are thought to be stable against Li. For example, LiPON, which is calculated using Li_2PO_2N as a representative of the material class (details are provided in the Supporting Information), shows a reduction potential of 0.69 V. The final decomposition products of LiPON in equilibrium with Li metal are Li_3N, Li_2O, and Li_3P (Table 2), which are consistent with the in situ XPS observations.[13] Although the calculated decomposition energy of LiPON is as large as −0.66 eV/atom at 0 V (Figure 1b and Table 2), LiPON is known to be compatible with Li metal as demonstrated by many experimental studies.[10,29] Similarly, Li_3PS_4 and $Li_7P_2S_8I$, which are reported to be compatible with Li metal anode,[8,30,31] are reduced against Li metal and at low voltages (Table 1 and Table 2). Therefore, the stability of these solid electrolyte materials against Li metal is not thermodynamically intrinsic.

The decomposition products, which form an interphase between the solid electrolyte and electrode, passivate the solid electrolyte and inhibit the continuous decomposition. For example, the decomposition products of LiPON, Li_3PS_4, and $Li_7P_2S_8I$ are Li binary compounds, such as Li_2O, Li_2S, Li_3P, Li_3N, and LiI, formed at the Li reduction. The interphase consisting of these decomposition products are stable against the high μ_{Li} of Li metal (Figure 2a), which is beyond the

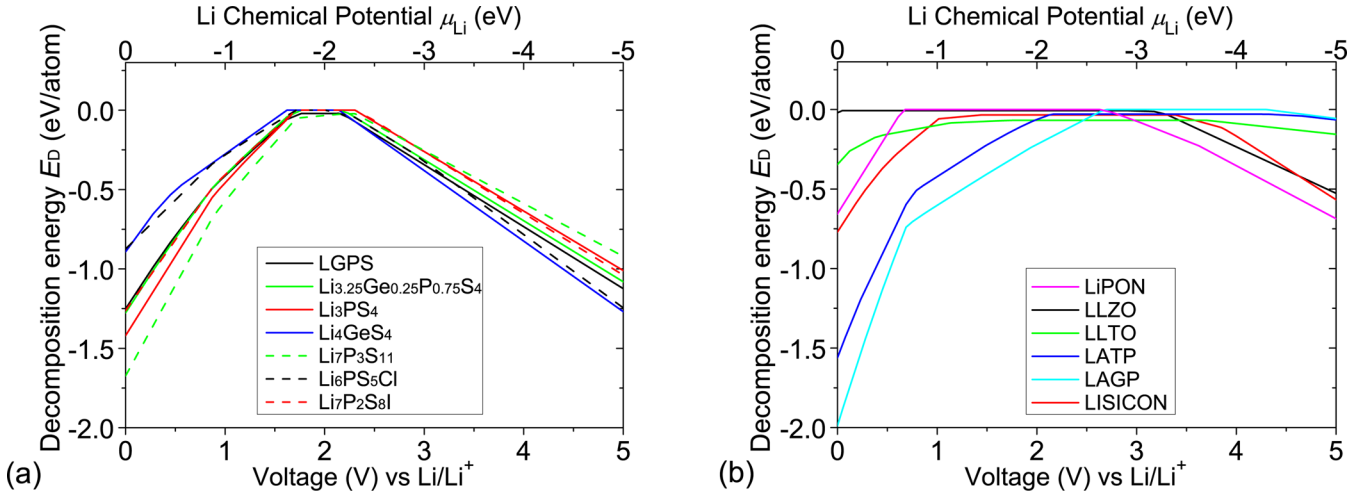

Figure 1. Decomposition energy E_D of (a) sulfide and (b) oxide solid electrolyte materials as a function of the applied voltage ϕ or Li chemical potential μ_{Li}.

DOI: 10.1021/acsami.5b07517
ACS Appl. Mater. Interfaces 2015, 7, 23685−23693

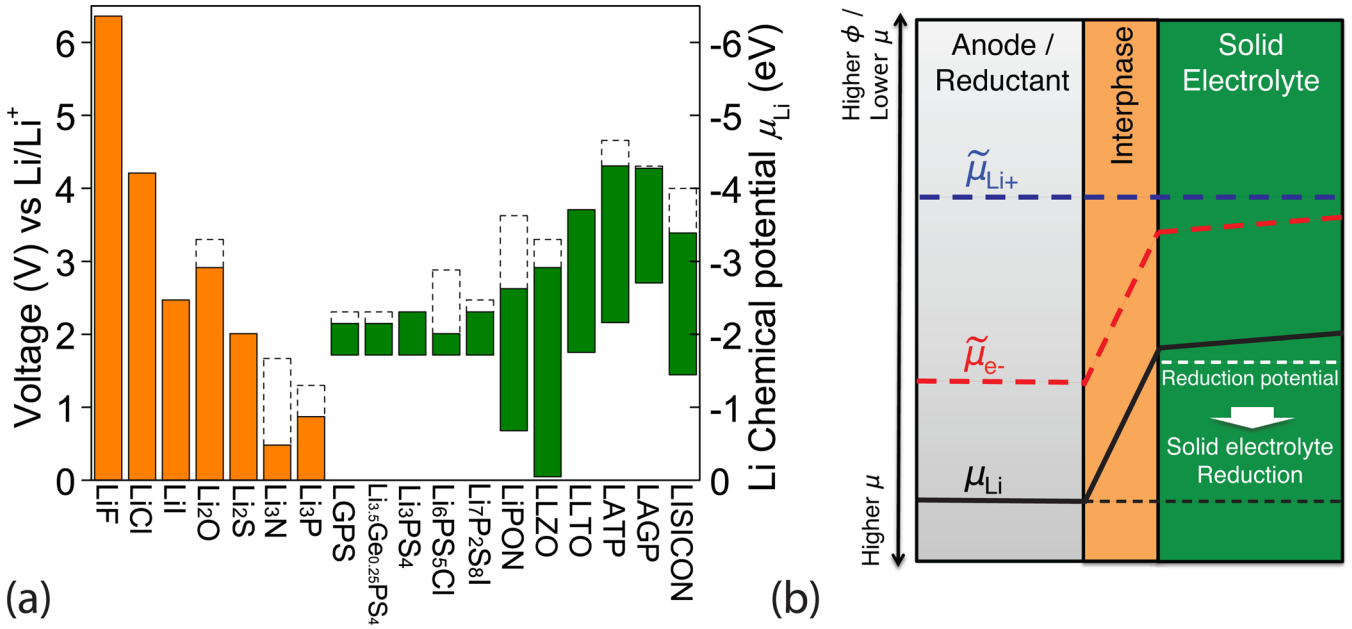

Figure 2. (a) Electrochemical window (solid color bar) of solid electrolyte and other materials. The oxidation potential to fully delithiate the material is marked by the dashed line. (b) Schematic diagram about the change of Li chemical potentials μ_{Li} (black line), the electrochemical potential $\tilde{\mu}_{Li^+}$ (blue dashed line), and $\tilde{\mu}_{e^-}$ (red dashed line) across the interface between the anode and the solid electrolyte. Since the actual profile of $\tilde{\mu}_{e^-}$ determined by the charge carrier distribution may be complicated,[32,33] the profiles of chemical and electrochemical potential shown here are schematic and may not be linear. The vertical scale is for the electrostatic potential or the voltage referenced to Li metal and is reversed for the chemical potential or electrochemical potential (eq 1).

reduction potential (cathodic limit) of the solid electrolyte (Figure 2b). At the equilibrium, the redistribution of Li^+ and other charged carriers (such as electron e^-) are formed at the interface to account for the potential drop across the electrode−electrolyte interface.[34] The electrochemical potential of the highly mobile Li^+, $\tilde{\mu}_{Li^+}$, which includes the electrostatic potential energy, is constant across the interface. In contrast, the electrochemical potential of the electronic carrier $\tilde{\mu}_{e^-}$, (red line in Figure 2b) decreases significantly in the interphase from the anode to the solid electrolyte, since these interphases have poor electronic mobility and conductivity. Therefore, the Li chemical potential μ_{Li} (black line in Figure 2b), which equals to the sum of $\tilde{\mu}_{Li^+}$ and $\tilde{\mu}_{e^-}$, decreases in the interphase from the anode to the solid electrolyte. The high value of μ_{Li} from the anode decreases to be within the electrochemical window of the solid electrolyte after the passivation of the decomposition interphase. As a result, the decomposition of the solid electrolyte has no thermodynamic driving force to continue into the bulk. The solid electrolyte is stabilized by the decomposition interphases, which essentially serve as solid-electrolyte-interphases (SEIs) in all-solid-state Li-ion batteries. In summary, the SEI of the decomposition interphase decreases the high Li chemical potential μ_{Li} applied on the solid electrolyte and bridges the Li chemical potential gap between Li metal and the solid electrolyte. This passivation mechanism explained the observed Li metal compatibility of LiPON, Li_3PS_4, and $Li_7P_2S_8I$.

The passivation mechanism relies on the electronic insulating properties of the decomposition interphase layers to stabilize the solid electrolyte and is not active if the interphase layer is electronically conductive. For example, the reduction of LGPS, LAGP, and LISICON with Li metal forms electronically conductive Li−Ge alloys, and the lithiation of LLTO and LATP forms titanates with Ti of 3+ or lower valences. The decomposition interphases for these solid electrolytes at Li reductions are mixed electronic and ionic conductors. The electronic conductivity in the interphase cannot account for the drop of $\tilde{\mu}_{e^-}$ across the interface regardless of the specific electron transport mechanism being metallic, band, or polaronic conduction. These mixed conductor interphases cannot account for the μ_{Li} drop as the change of both $\tilde{\mu}_{Li^+}$ and $\tilde{\mu}_{e^-}$ would be small across the interphase. As a result, the solid electrolyte is still exposed to the high μ_{Li} of the anode, and the reduction reaction continues into the bulk. In addition, the mixed electronic and ionic conductor interphase facilitate the kinetic transport of Li ion and electrons for the decomposition reactions.[14] The absence of the passivation mechanism explains the lithation and reduction of LGPS, LLTO, LATP, LAGP, and LISICON observed in the CV experiments.

It is worth noting that garnet LLZO shows the lowest reduction potential of as low as 0.05 V against Li and the least favorable decomposition reaction energy of only 0.021 eV/atom (49 kJ/mol of LLZO) at 0 V among all solid electrolyte materials examined (Figure 1 and Table 2). Given such small reaction energy, the Li reduction of garnet is likely to be kinetically inhibited, and the reduction products of Li_2O, Zr_3O, and La_2O_3 (Table 1) may provide passivation to the material. These explain the widely reported 0−5 V window of garnet from the CV measurements in the literature.[5,35] The reduction of garnet at 0.05 V forms Zr_3O (Table 1), following another plateau at 0.004 V to form Zr (Table 2 and Table S2) based on the DFT GGA energies. Since these small values of energy and voltage is below typical accuracy of DFT and the approximations of the scheme (see section 2), it is inconclusive whether the garnet LLZO is reduced to Zr_3O or Zr at 0 V or against Li metal. Nevertheless, the formation of Zr would be thermodynamically favorable at a potential significantly lower than 0 V, which corresponds to applying high current density at

DOI: 10.1021/acsami.5b07517
ACS Appl. Mater. Interfaces 2015, 7, 23685−23693

the Li−LLZO interface. Recent report of instability of garnet against Li at elevated temperatures of 300 °C may be an indication of the limited stability of garnet against Li metal,[36] as the diffusion and phase nucleation are facilitated at high temperatures.

3.2. Stability of Solid Electrolyte Materials at High Voltages. The oxidation reactions of the solid electrolyte materials were investigated using the same method in section 3.1. The LGPS material is delithiated and oxidized starting at 2.14 V (Table 1 and Figure 1), and the final oxidation products of P_2S_5, GeS_2, and S are formed at the equilibrium oxidation potential of 2.31 V (Table 3). The oxidation potential of the LGPS is confirmed by the CV experiment.[12] Similar to Li_2S, all sulfide solid electrolytes such as $Li_{3.25}Ge_{0.25}P_{0.75}S_4$, Li_3PS_4, Li_4GeS_4, $Li_7P_3S_{11}$, and $Li_7P_2S_8I$ are oxidized at 2−2.5 V to form S (Table 1 and Table 3). The other elements, such as P and Ge, are usually oxidized into P_2S_5 and GeS_2, respectively. The oxidation reactions of sulfide solid electrolytes are highly favorable at 5 V as described by the decomposition energy (Figure 1a and Table 3).

Table 3. Oxidation Reaction of the Solid Electrolyte Materials at 5 V

	phase equilibria at 5 V	E_D (eV/atom)
Li_2S	S	−1.99
LGPS	GeS_2, P_2S_5, S	−1.12
$Li_{3.25}Ge_{0.25}P_{0.75}S_4$	P_2S_5, S, GeS_2	−1.08
Li_3PS_4	S, P_2S_5	−1.01
Li_4GeS_4	GeS_2, S	−1.27
$Li_7P_3S_{11}$	S, P_2S_5	−0.92
Li_6PS_5Cl	P_2S_5, S, PCl_3	−1.33
$Li_7P_2S_8I$	P_2S_5, S, I_2	−1.04
LiPON	PNO, P_2O_5, N_2	−0.69
LLZO	O_2, La_2O_3, $La_2Zr_2O_7$	−0.53
LLTO	O_2, TiO_2, $La_2Ti_2O_7$	−0.15
LATP	O_2, TiP_2O_7, $Ti_5P_4O_{20}$, $AlPO_4$	−0.065
LAGP	$Ge_5O(PO_4)_6$, GeP_2O_7, $AlPO_4$, O_2	−0.056
LISICON	Zn_2GeO_4, GeO_2, O_2	−0.57

Oxide solid electrolyte materials have higher oxidation potential than sulfides. The oxidation of LLZO, LISICON, and LLTO starts at 2.91, 3.39, and 3.71 V, respectively. The NASICON materials, LATP and LAGP, show the best resistance to oxidation with the highest oxidation potential of 4.21 and 4.28 V, respectively (Table 1), and the lowest decomposition energy of only ∼−0.06 eV/atom at 5 V (Figure 1b and Table 3). The delithiation reactions continue at higher voltages, and O_2 gas is released during the oxidation at high voltages for all oxide solid electrolytes (Table 3). The oxidation of these solid electrolyte materials is not surprising, given that Li_2O is oxidized at 2.9 V and that the O_2 gas is released by the further oxidation of Li_2O_2. LiPON starts oxidation at 2.63 V with the N_2 gas release. Our computation results are consistent with the experiments by Yu et al.,[10] in which the onset of LiPON oxidation at ∼2.6 V in the $I-V$ measurements and the microsized gas bubbles in the LiPON material were observed after applying a high voltage of 6 V.

A significant overpotential to the calculated thermodynamic equilibrium potential is expected for the oxidation reaction processes, which are likely to have slow kinetics. The kinetic limitations of the oxidation reactions may come from multiple aspects. Most decomposition products at high voltages (Table 3) are electronically insulating, and the diffusion of non-Li elements is usually slow in solids. Furthermore, the nucleation and release of O_2 and N_2 gas molecules are likely to have sluggish kinetics. For example, a significant overpotential of >1 V is often observed in the oxygen evolution reactions in metal-air batteries.[37] Therefore, the overpotential of the decomposition reactions may provide a higher nominal oxidation potential of >5 V and a wider nominal electrochemical window observed in the CV experiments.[1,8−10]

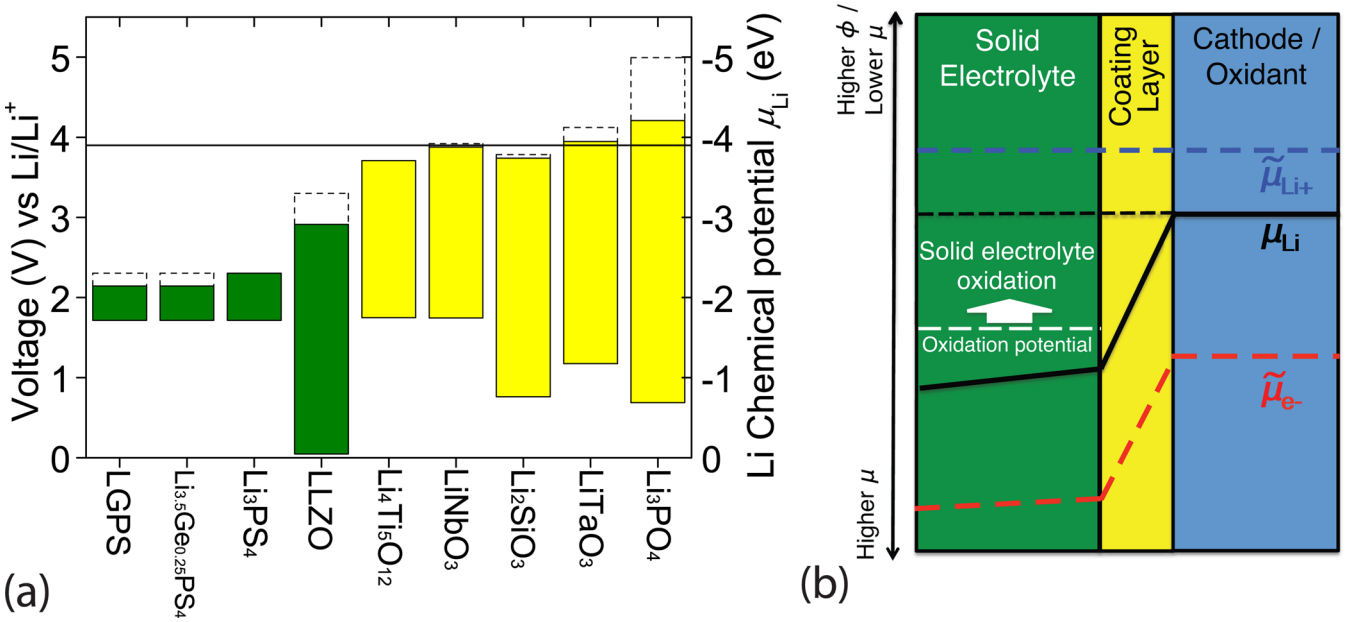

Figure 3. (a) Electrochemical stability window (solid color bars) of commonly used coating layer materials. The oxidation potential to fully delithiate the material is marked by the dashed line. The line at 3.9 V represents the equilibrium voltage of the $LiCoO_2$ cathode material. (b) Schematic diagram about the change of Li chemical potentials μ_{Li} (black line) and the electrochemical potential $\tilde{\mu}_{Li^+}$ (blue dashed line) and $\tilde{\mu}_{e^-}$ (red dashed line) across the interface between the solid electrolyte and the cathode material.

DOI: 10.1021/acsami.5b07517
ACS Appl. Mater. Interfaces 2015, 7, 23685−23693

3.3. Extend the Stability of Solid Electrolytes by Applying Coating Layers. Currently, the interfacial resistance has become a critical problem for the performance of all-solid-state Li-ion batteries. The engineering of the interface, such as the application of interfacial coating layers, is used to improve interfacial protection and to reduce interface resistance. In this section, we investigated the electrochemical stability of the coating layer materials, such as $Li_4Ti_5O_{12}$,[38,39] $LiTaO_3$,[40] $LiNbO_3$,[41,42] Li_2SiO_3,[43] and Li_3PO_4,[44] which were demonstrated to suppress the mutual diffusion of non-Li elements and to reduce the interfacial resistance at the solid electrolyte−cathode interfaces in all-solid-state Li-ion batteries.[2,16,40,45] Our calculations show that these coating layer materials have an electrochemical window from the reduction potential of 0.7−1.7 V to the oxidation potential of 3.7−4.2 V (Figure 3a). Therefore, the coating layer materials are stable between 2 and 4 V, the usual voltage range during the cycling of Li-ion batteries. In addition, the coating layer materials have poor electronic conductivity and can serve as artificial SEIs to passivate the solid electrolyte through the same mechanisms illustrated in section 3.1 (Figure 3b). Given that the sulfide solid electrolyte materials are oxidized at as low as 2 V and are not thermodynamically stable at the voltage of 4 V, the coating layers serve as critical passivations through the same mechanism illustrated in section 3.1. The coating layers mitigate the low Li chemical potential μ_{Li} from the cathode material applied on the solid electrolyte materials. As a result, the oxidation and delithiation of the solid electrolyte at the cathode interface is stopped, and the oxidation potential (anodic limit) of the solid electrolyte is extended by the artificial coating layer. Therefore, the coating layer effectively extended the anodic limit of the sulfide solid electrolyte from ∼2−2.3 V to ∼4 V. The overpotential to oxidize the coating layers may further extend the nominal stability window. Similar strategy of applying artificial coating layers has been employed at the anode side for the protection and stabilization of Li metal anode. For example, Polyplus[46] has applied coating layers between Li metal and LATP electrolyte to protect the LATP materials against Li metal. The passivation mechanism of the coating layer at the anode side is the same as the decomposition interphase demonstrated in section 3.1.

4. DISCUSSION

Our thermodynamic analyses based on first-principles calculations indicate that most solid electrolyte materials have a limited electrochemical window. In contrast to the widely held perception about the outstanding stability of the solid electrolyte materials, the solid electrolyte materials are reduced and oxidized at low and high potentials, respectively, and are not thermodynamically stable against Li metal. The sulfide solid electrolytes based on thio-phosphates are reduced at ∼1.6−1.7 V and oxidized at ∼2−2.3 V. The stability window of oxide solid electrolytes varies greatly from one material to another. Although some oxides have high reduction potential as sulfides, most oxide solid electrolytes have a significantly higher oxidation potential and are not oxidized until >3 V. In particular, the NASICON materials, LATP and LAGP, are thermodynamically stable up to ∼4.2 V. Among all these oxides investigated, the Li garnet materials, such as LLZO, have the best resistance to Li reduction. Overall, the oxide solid electrolyte materials have significantly wider electrochemical window than sulfides. The reduction and oxidation potentials as well as the decomposition products of solid electrolytes predicted from our calculations are in good agreement with prior experimental studies, confirming that our computation method based on the Li grand potential phase diagram is a valid scheme in evaluating the electrochemical stability of materials.

Our calculation results demonstrated that the good stability of the solid electrolyte materials is originated from the kinetic stabilizations. First, the wide, nominal electrochemical window observed in many CV experiments can be partially attributed to the significant overpotential of the sluggish kinetics during the decomposition reactions (Figure 4). The decomposition

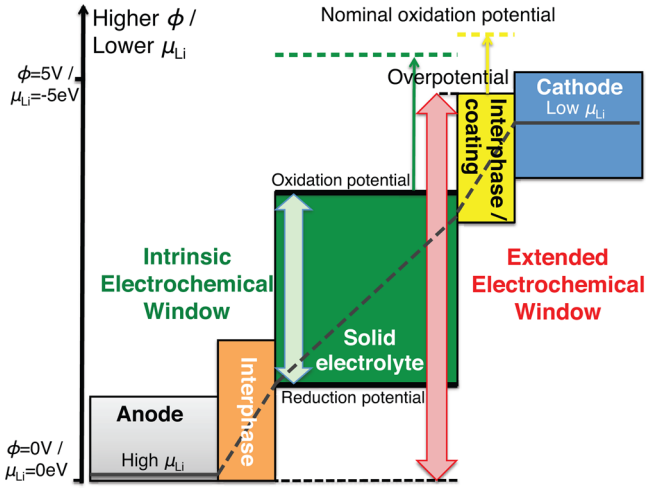

Figure 4. Schematic diagram about the electrochemical window (color bars) and the Li chemical potential profile (black line) in the all-solid-state Li-ion battery. The profile of chemical potential is schematic in this plot and may not be linear. The high μ_{Li} in the anode (silver) and low μ_{Li} in the cathode (blue) are beyond the stability window of the solid electrolyte (green). The observed nominal electrochemical window is extended by the overpotential (dashed line) and by the interphases (orange and yellow), which account for the gap of μ_{Li} between solid electrolyte and electrodes across the interfaces.

reactions though kinetically sluggish are still thermodynamically favorable at the applied overpotential and may happen over an extended period of time, leading to the deterioration of the batteries. This kinetic stabilization from the sluggish kinetics of the reactions is different from the passivation mechanisms illustrated in section 3.1. The passivation mechanism of the interphases is the origin of the outstanding stability in the solid electrolyte. The decomposition interphases with good stability and poor electronic transport are effectively the SEIs in the all-solid-state Li-ion batteries to passivate the solid electrolytes (Figure 4). The interphases, which are stable against solid electrolytes and electrodes, mitigate the Li chemical potential discrepancy between the electrolyte and electrode at the interfaces. As a result, the anodic/cathode limits and the electrochemical window of the solid electrolyte are significantly extended by the extra electrochemical window provided by the interphases (Figure 4). The effective electrochemical window of the solid electrolyte materials is its own intrinsic electrochemical window plus the electrochemical window of the interphases (Figure 4).

In this study, the electrochemical window of the solid electrolyte and the extensions by the interphases were calculated using the first-principles methods. Our computation scheme evaluated the electrochemical window based on the equilibrium of the neutral Li, which is a necessary condition for

DOI: 10.1021/acsami.5b07517
ACS Appl. Mater. Interfaces 2015, 7, 23685−23693

the equilibrium at the interface. As suggested by Good-enough,[47] the electrochemical window of the electrolyte can also be estimated by the difference between the lowest unoccupied molecular orbital (LUMO) and highest occupied molecular orbital (HOMO) states of the electrolyte based on the equilibrium of electrons across the interfaces. These equilibrium conditions of carriers other than neutral Li also need to be satisfied at the interfaces. The equilibria of the charged carriers such as electrons or Li^+ are subject to the formation of polarizations and interfacial space charge layers, which are dependent on the defect chemistry and the structures of the interface.[32,33] In some cases, a significant amount of electrons or holes may accumulate in the interphases due to the charge redistribution, defect chemistry, or special interfacial structures and may activate the electronic conductions in the interphase deactivating the passivation effects. Nevertheless, our results based on the equilibrium of neutral Li are in good agreement with many experimental studies, suggesting the validity of our scheme.

The interphase stabilization mechanism provides guidance for the development of solid electrolyte materials. The formation of the decomposition interphases plays an essential role in the stability of the solid electrolyte and should be considered in the design of solid electrolyte materials. Our calculations have shown that the reduction of the solid electrolytes is generally governed by the reduction of the cations, and the interphases formed by the reduction of these cations often control the interfacial stability. For example, LGPS, LAGP, LATP, and LLTO solid electrolyte materials form electronically conductive interphases at low voltages, such as Li−Ge alloys or Li titanates, which cannot provide the passivation for the solid electrolyte materials. Therefore, our results suggest that certain cations or dopants, such as Ti and Ge, in the solid electrolyte materials, negatively affect the stability against Li metal. Other cations, such as Si, Sn, Al, and Zn, may have a similar effect. However, doping with anions does not have such limitations for the stability of the solid electrolyte at low voltages. The Li reduction products of common anions, such as O, S, F, Cl, and I, are usually Li binary materials, such as lithium chalcogenides and lithium halides, which are thermodynamically stable against Li and are good electronic insulators. The passivation provided by these materials is the origin of Li metal compatibility for LiPON, Li_3PS_4, and $Li_7P_2S_8I$ solid electrolyte materials.[8,10,13,30] Doping lithium halides is a highly effective method in the design of solid electrolyte to simultaneously achieve improved ionic conductivity and Li metal stability.[30,48,49]

In addition, the properties of the decomposition interphases significantly affect the performance of all-solid-state Li-ion batteries. The decomposition interphases with electronic conductivity may enable the continuous decomposition of the solid electrolyte during the cycling of the batteries. For example, a recent experimental study[12] has identified that the reduction and oxidation products of the LGPS can be reversibly cycled. Therefore, the interphases formed due to the decomposition of the solid electrolyte may effectively become a part of active electrode materials of the battery. Such decomposition of the solid electrolyte materials during the cycling of the battery may cause degradations of the interfaces, leading to high interfacial resistance, low coulombic efficiency, and poor reversibility, which are major limiting factors in the performance of all-solid-state Li-ion batteries. While the good electronic insulation of the decomposition products are preferred to achieve good stability and low thickness of the interphases, the high Li ionic conductivity is important for achieving low interfacial resistance. For example, Li_3N and Li_3P formed at the LiPON−Li interface are phases with high Li ionic conductivity,[50,51] which may explain the good interfacial conductance for LiPON−Li interface.

However, the properties of the decomposition interphases may not always be as desired, since these critical interfacial properties are determined by the spontaneous decomposition of the solid electrolytes and electrode materials.[16] The undesired electronic conductivity of the decomposition products may cause continuous decompositions of the solid electrolyte materials, since the electronic insulation of the decomposition interphases is essential in stabilizing the solid electrolyte. The engineering of the interface, such as the application of artificial coating layer, is a demonstrated method for the interfacial protection and to reduce interfacial resistance if the spontaneously formed SEI layers have unsatisfactory properties (e.g., high electronic conductivity and low Li^+ conductivity). Our calculation results showed that the coating layer materials passivate the solid electrolyte against the oxidation at high voltages. The outstanding stability of the coating layer against both solid electrolyte and electrode also impedes the mutual diffusion of non-Li elements, such as Co and S, at the interface, which is a known problem for the degradation of interfaces between the sulfide electrolyte and $LiCoO_2$.[16] Furthermore, the coating layer artificially applied through thin film deposition is as thin as a few nanometers,[38,42] while the interphase layer formed by the spontaneous decomposition can be as thick as 100 nm.[16,42,45] The thinner coating layer of less than 10 nm yields significantly lower interfacial resistance.[16,42] In addition, as the applied coating layer bridges the differences of Li chemical potential between the solid electrolyte and the cathode material, the formation of space-charge layers is mitigated[40] to reduce the interfacial resistance. Therefore, applying artificial coating layer provides multiple advantages compared to the interphases formed by the spontaneous decompositions. The development of materials processing techniques to engineer the interphases is critical for improving the performance of all-solid-state Li-ion batteries.

5. CONCLUSIONS

Our first-principles calculation results indicate that most solid electrolyte materials have limited electrochemical window in contrast to the widely held perception about the outstanding stability of the solid electrolyte materials. Most solid electrolyte materials are not thermodynamically stable against Li metal and are reduced and oxidized at low and high potentials, respectively. Sulfide-based solid electrolytes have significantly narrower electrochemical window than the oxide-based solid electrolytes. Our calculation results show that the good stability of the solid electrolyte materials is not thermodynamically intrinsic but is rather originated from the kinetic stabilization. This kinetic stabilization is achieved due to the sluggish kinetics of the decomposition reactions and the decomposition interphases with poor electronic transport similar to the SEIs. We illustrated the stabilization mechanisms of the decomposition interphases, which passivate the solid electrolytes by mitigating extreme Li chemical potential from the electrodes. Our results suggest that the decomposition interphases of the solid electrolyte and the engineering of the interface are critical for the performance of all-solid-state Li-ion batteries. The interphases with good electronic insulation and high Li ionic

DOI: 10.1021/acsami.5b07517
ACS Appl. Mater. Interfaces 2015, 7, 23685−23693

conductivity are preferred to achieve an interface with good stability and low resistance. The application of artificial coating layers is a promising method for the stabilizing interfaces and for reducing interfacial resistance. Our study demonstrated the computation scheme to evaluate the electrochemical stability and the decomposition interphases of solid electrolyte materials and provided the fundamental understanding to guide the future design of solid electrolytes and interphases in all-solid-state Li-ion batteries.

■ ASSOCIATED CONTENT

Supporting Information

The Supporting Information is available free of charge on the ACS Publications website at DOI: 10.1021/acsami.5b07517.

Descriptions about the solid electrolyte materials investigated in the computation and the calculated phase equilibria for the lithiation and delithiation of solid electrolyte and coating materials (PDF)

■ AUTHOR INFORMATION

Corresponding Author

*E-mail: yfmo@umd.edu.

Notes

The authors declare no competing financial interest.

■ ACKNOWLEDGMENTS

We thank Prof. Chunsheng Wang and Fudong Han for helpful discussions. This work was supported by U.S. Department of Energy, Office of Energy Efficiency and Renewable Energy, under Award No. DE-EE0006860. This research used computational facilities from the University of Maryland supercomputing resources and from the Extreme Science and Engineering Discovery Environment (XSEDE) supported by National Science Foundation Award No. TG-DMR130142.

■ REFERENCES

(1) Kamaya, N.; Homma, K.; Yamakawa, Y.; Hirayama, M.; Kanno, R.; Yonemura, M.; Kamiyama, T.; Kato, Y.; Hama, S.; Kawamoto, K.; Mitsui, A. A Lithium Superionic Conductor. *Nat. Mater.* **2011**, *10*, 682−686.

(2) Takada, K. Progress and Prospective of Solid-State Lithium Batteries. *Acta Mater.* **2013**, *61*, 759−770.

(3) Seino, Y.; Ota, T.; Takada, K.; Hayashi, A.; Tatsumisago, M. A Sulphide Lithium Super Ion Conductor Is Superior to Liquid Ion Conductors for Use in Rechargeable Batteries. *Energy Environ. Sci.* **2014**, *7*, 627−631.

(4) Yamane, H.; Shibata, M.; Shimane, Y.; Junke, T.; Seino, Y.; Adams, S.; Minami, K.; Hayashi, A.; Tatsumisago, M. Crystal Structure of a Superionic Conductor, Li7P3S11. *Solid State Ionics* **2007**, *178*, 1163−1167.

(5) Thangadurai, V.; Pinzaru, D.; Narayanan, S.; Baral, A. K. Fast Solid-State Li Ion Conducting Garnet-Type Structure Metal Oxides for Energy Storage. *J. Phys. Chem. Lett.* **2015**, *6*, 292−299.

(6) Li, J.; Baggetto, L.; Martha, S. K.; Veith, G. M.; Nanda, J.; Liang, C.; Dudney, N. J. An Artificial Solid Electrolyte Interphase Enables the Use of a LiNi0.5Mn1.5O4 5 V Cathode with Conventional Electrolytes. *Adv. Energy Mater.* **2013**, *3*, 1275−1278.

(7) Li, J.; Ma, C.; Chi, M.; Liang, C.; Dudney, N. J. Solid Electrolyte: The Key for High-Voltage Lithium Batteries. *Adv. Energy Mater.* **2015**, *5*, 1401408.

(8) Liu, Z.; Fu, W.; Payzant, E. A.; Yu, X.; Wu, Z.; Dudney, N. J.; Kiggans, J.; Hong, K.; Rondinone, A. J.; Liang, C. Anomalous High Ionic Conductivity of Nanoporous Beta-Li3PS4. *J. Am. Chem. Soc.* **2013**, *135*, 975−978.

(9) Thangadurai, V.; Weppner, W. Li6ALa2Ta2O12 (a = Sr, Ba): Novel Garnet-Like Oxides for Fast Lithium Ion Conduction. *Adv. Funct. Mater.* **2005**, *15*, 107−112.

(10) Yu, X.; Bates, J. B.; Jellison, G. E.; Hart, F. X. A Stable Thin - Film Lithium Electrolyte: Lithium Phosphorus Oxynitride. *J. Electrochem. Soc.* **1997**, *144*, 524−532.

(11) Mo, Y.; Ong, S. P.; Ceder, G. First Principles Study of the Li10GeP2S12 Lithium Super Ionic Conductor Material. *Chem. Mater.* **2012**, *24*, 15−17.

(12) Han, F.; Gao, T.; Zhu, Y.; Gaskell, K. J.; Wang, C. A Battery Made from a Single Material. *Adv. Mater.* **2015**, *27*, 3473−3483.

(13) Schwöbel, A.; Hausbrand, R.; Jaegermann, W. Interface Reactions between LiPON and Lithium Studied by in-Situ X-Ray Photoemission. *Solid State Ionics* **2015**, *273*, 51−54.

(14) Wenzel, S.; Leichtweiss, T.; Krüger, D.; Sann, J.; Janek, J. Interphase Formation on Lithium Solid Electrolytes—an in Situ Approach to Study Interfacial Reactions by Photoelectron Spectroscopy. *Solid State Ionics* **2015**, *278*, 98−105.

(15) Hartmann, P.; Leichtweiss, T.; Busche, M. R.; Schneider, M.; Reich, M.; Sann, J.; Adelhelm, P.; Janek, J. Degradation of NASICON-Type Materials in Contact with Lithium Metal: Formation of Mixed Conducting Interphases (MCI) on Solid Electrolytes. *J. Phys. Chem. C* **2013**, *117*, 21064−21074.

(16) Sakuda, A.; Hayashi, A.; Tatsumisago, M. Interfacial Observation between LiCoO2 Electrode and Li2S−P2S5 Solid Electrolytes of All-Solid-State Lithium Secondary Batteries Using Transmission Electron Microscopy. *Chem. Mater.* **2010**, *22*, 949−956.

(17) Jain, A.; Hautier, G.; Moore, C. J.; Ping Ong, S.; Fischer, C. C.; Mueller, T.; Persson, K. A.; Ceder, G. A High-Throughput Infrastructure for Density Functional Theory Calculations. *Comput. Mater. Sci.* **2011**, *50*, 2295−2310.

(18) Wang, L.; Maxisch, T.; Ceder, G. Oxidation Energies of Transition Metal Oxides within the GGA+U Framework. *Phys. Rev. B: Condens. Matter Mater. Phys.* **2006**, *73*, 195107.

(19) Jain, A.; Hautier, G.; Ong, S. P.; Moore, C. J.; Fischer, C. C.; Persson, K. A.; Ceder, G. Formation Enthalpies by Mixing GGA and GGA+U Calculations. *Phys. Rev. B: Condens. Matter Mater. Phys.* **2011**, *84*, 045115.

(20) Jain, A.; Ong, S. P.; Hautier, G.; Chen, W.; Richards, W. D.; Dacek, S.; Cholia, S.; Gunter, D.; Skinner, D.; Ceder, G.; Persson, K. A. Commentary: The Materials Project: A Materials Genome Approach to Accelerating Materials Innovation. *APL Mater.* **2013**, *1*, 011002.

(21) Ong, S. P.; Wang, L.; Kang, B.; Ceder, G. Li−Fe−P−O2 Phase Diagram from First Principles Calculations. *Chem. Mater.* **2008**, *20*, 1798−1807.

(22) Ong, S. P.; Richards, W. D.; Jain, A.; Hautier, G.; Kocher, M.; Cholia, S.; Gunter, D.; Chevrier, V. L.; Persson, K. A.; Ceder, G. Python Materials Genomics (Pymatgen): A Robust, Open-Source Python Library for Materials Analysis. *Comput. Mater. Sci.* **2013**, *68*, 314−319.

(23) Ong, S. P.; Mo, Y.; Richards, W. D.; Miara, L.; Lee, H. S.; Ceder, G. Phase Stability, Electrochemical Stability and Ionic Conductivity of the $Li_{10\pm1}MP_2X_{12}$ (M = Ge, Si, Sn, Al or P, and X = O, S or Se) Family of Superionic Conductors. *Energy Environ. Sci.* **2013**, *6*, 148−156.

(24) Chen, C. H.; Amine, K. Ionic Conductivity, Lithium Insertion and Extraction of Lanthanum Lithium Titanate. *Solid State Ionics* **2001**, *144*, 51−57.

(25) Stramare, S.; Thangadurai, V.; Weppner, W. Lithium Lanthanum Titanates: A Review. *Chem. Mater.* **2003**, *15*, 3974−3990.

(26) Feng, J. K.; Lu, L.; Lai, M. O. Lithium Storage Capability of Lithium Ion Conductor Li1.5Al0.5Ge1.5(PO4)3. *J. Alloys Compd.* **2010**, *501*, 255−258.

(27) Alpen, U. v.; Bell, M. F.; Wichelhaus, W.; Cheung, K. Y.; Dudley, G. J. Ionic Conductivity of Li14Zn(GeO4)4 (LISICON). *Electrochim. Acta* **1978**, *23*, 1395−1397.

(28) Knauth, P. Inorganic Solid Li Ion Conductors: An Overview. *Solid State Ionics* **2009**, *180*, 911−916.

DOI: 10.1021/acsami.5b07517
ACS Appl. Mater. Interfaces 2015, 7, 23685−23693

(29) West, W. C.; Whitacre, J. F.; Lim, J. R. Chemical Stability Enhancement of Lithium Conducting Solid Electrolyte Plates Using Sputtered LiPON Thin Films. *J. Power Sources* **2004**, *126*, 134−138.
(30) Rangasamy, E.; Liu, Z.; Gobet, M.; Pilar, K.; Sahu, G.; Zhou, W.; Wu, H.; Greenbaum, S.; Liang, C. An Iodide-Based Li7P2S8I Superionic Conductor. *J. Am. Chem. Soc.* **2015**, *137*, 1384−1387.
(31) Lepley, N. D.; Holzwarth, N. A. W.; Du, Y. A. Structures, Li+ Mobilities, and Interfacial Properties of Solid Electrolytes Li3PS4 and Li3PO4 from First Principles. *Phys. Rev. B: Condens. Matter Mater. Phys.* **2013**, *88*, 104103.
(32) Leung, K.; Leenheer, A. How Voltage Drops Are Manifested by Lithium Ion Configurations at Interfaces and in Thin Films on Battery Electrodes. *J. Phys. Chem. C* **2015**, *119*, 10234−10246.
(33) Haruyama, J.; Sodeyama, K.; Han, L.; Takada, K.; Tateyama, Y. Space−Charge Layer Effect at Interface between Oxide Cathode and Sulfide Electrolyte in All-Solid-State Lithium-Ion Battery. *Chem. Mater.* **2014**, *26*, 4248−4255.
(34) Weppner, W., Fundamental Aspects of Electrochemical, Chemical and Electrostatic Potentials in Lithium Batteries. In *Materials for Lithium-Ion Batteries*; Julien, C., Stoynov, Z., Eds.; Springer Netherlands: Dordrecht, The Netherlands, 2000; Chapter 20, pp 401−412.
(35) Kotobuki, M.; Munakata, H.; Kanamura, K.; Sato, Y.; Yoshida, T. Compatibility of Li7La3Zr2O12 Solid Electrolyte to All-Solid-State Battery Using Li Metal Anode. *J. Electrochem. Soc.* **2010**, *157*, A1076−A1079.
(36) Wolfenstine, J.; Allen, J. L.; Read, J.; Sakamoto, J. Chemical Stability of Cubic Li7La3Zr2O12 with Molten Lithium at Elevated Temperature. *J. Mater. Sci.* **2013**, *48*, 5846−5851.
(37) McCloskey, B. D.; Scheffler, R.; Speidel, A.; Girishkumar, G.; Luntz, A. C. On the Mechanism of Nonaqueous Li−O2 Electrochemistry on C and Its Kinetic Overpotentials: Some Implications for Li−Air Batteries. *J. Phys. Chem. C* **2012**, *116*, 23897−23905.
(38) Ohta, N.; Takada, K.; Zhang, L.; Ma, R.; Osada, M.; Sasaki, T. Enhancement of the High-Rate Capability of Solid-State Lithium Batteries by Nanoscale Interfacial Modification. *Adv. Mater.* **2006**, *18*, 2226−2229.
(39) Kitaura, H.; Hayashi, A.; Tadanaga, K.; Tatsumisago, M. Improvement of Electrochemical Performance of All-Solid-State Lithium Secondary Batteries by Surface Modification of LiMn2O4 Positive Electrode. *Solid State Ionics* **2011**, *192*, 304−307.
(40) Takada, K.; Ohta, N.; Zhang, L.; Fukuda, K.; Sakaguchi, I.; Ma, R.; Osada, M.; Sasaki, T. Interfacial Modification for High-Power Solid-State Lithium Batteries. *Solid State Ionics* **2008**, *179*, 1333−1337.
(41) Ohta, N.; Takada, K.; Sakaguchi, I.; Zhang, L.; Ma, R.; Fukuda, K.; Osada, M.; Sasaki, T. LiNbO3-Coated LiCoO2 as Cathode Material for All Solid-State Lithium Secondary Batteries. *Electrochem. Commun.* **2007**, *9*, 1486−1490.
(42) Kato, T.; Hamanaka, T.; Yamamoto, K.; Hirayama, T.; Sagane, F.; Motoyama, M.; Iriyama, Y. In-Situ Li7La3Zr2O12/LiCoO2 Interface Modification for Advanced All-Solid-State Battery. *J. Power Sources* **2014**, *260*, 292−298.
(43) Sakuda, A.; Kitaura, H.; Hayashi, A.; Tadanaga, K.; Tatsumisago, M. Improvement of High-Rate Performance of All-Solid-State Lithium Secondary Batteries Using LiCoO2 Coated with Li2O−SiO2 Glasses. *Electrochem. Solid-State Lett.* **2008**, *11*, A1−A3.
(44) Jin, Y.; Li, N.; Chen, C. H.; Wei, S. Q. Electrochemical Characterizations of Commercial LiCoO2 Powders with Surface Modified by Li3PO4 Nanoparticles. *Electrochem. Solid-State Lett.* **2006**, *9*, A273−A276.
(45) Kim, K. H.; Iriyama, Y.; Yamamoto, K.; Kumazaki, S.; Asaka, T.; Tanabe, K.; Fisher, C. A. J.; Hirayama, T.; Murugan, R.; Ogumi, Z. Characterization of the Interface between LiCoO2 and Li7La3Zr2O12 in an All-Solid-State Rechargeable Lithium Battery. *J. Power Sources* **2011**, *196*, 764−767.
(46) Visco, S.; Nimon, V.; Petrov, A.; Pridatko, K.; Goncharenko, N.; Nimon, E.; De Jonghe, L.; Volfkovich, Y.; Bograchev, D. Aqueous and Nonaqueous Lithium-Air Batteries Enabled by Water-Stable Lithium Metal Electrodes. *J. Solid State Electrochem.* **2014**, *18*, 1443−1456.
(47) Goodenough, J. B.; Kim, Y. Challenges for Rechargeable Li Batteries. *Chem. Mater.* **2010**, *22*, 587−603.
(48) Rangasamy, E.; Li, J.; Sahu, G.; Dudney, N.; Liang, C. Pushing the Theoretical Limit of Li-CFx Batteries: A Tale of Bifunctional Electrolyte. *J. Am. Chem. Soc.* **2014**, *136*, 6874−6877.
(49) Deiseroth, H.-J.; Kong, S.-T.; Eckert, H.; Vannahme, J.; Reiner, C.; Zaiß, T.; Schlosser, M. Li6PS5X: A Class of Crystalline Li-Rich Solids with an Unusually High Li+ Mobility. *Angew. Chem., Int. Ed.* **2008**, *47*, 755−758.
(50) Alpen, U. v.; Rabenau, A.; Talat, G. H. Ionic Conductivity in Li3N Single Crystals. *Appl. Phys. Lett.* **1977**, *30*, 621−623.
(51) Nazri, G. Preparation, Structure and Ionic Conductivity of Lithium Phosphide. *Solid State Ionics* **1989**, *34*, 97−102.

DOI: 10.1021/acsami.5b07517
ACS Appl. Mater. Interfaces 2015, 7, 23685−23693